




# A New Helioseismic Constraint on a Cosmic-time Variation of $G$

Alfio Bonanno<sup>1</sup>  and Hans-Erich Fröhlich<sup>2</sup><sup>1</sup> INAF, Osservatorio Astrofisico di Catania, via S. Sofia, 78, I-95123 Catania, Italy<sup>2</sup> Leibniz Institute for Astrophysics Potsdam (AIP), An der Sternwarte 16, D-14482 Potsdam, Germany

Received 2020 February 20; revised 2020 April 3; accepted 2020 April 6; published 2020 April 21

## Abstract

The best available estimate of 8640 days of low- $\ell$  BiSON data is used to constrain the evolution of Newton’s constant over cosmic time. The effect of different chemical compositions and the impact of the theoretical uncertainties on the efficiency of the proton–proton ( $pp$ ) fusion cross-section have been considered within a Bayesian approach. The resulting new helioseismic limit on the variation of the gravitational constant turns out to be  $|\dot{G}/G|_{t=t_0} < 2 \times 10^{-13} \text{ yr}^{-1}$ .

*Unified Astronomy Thesaurus concepts:* Helioseismology (709); Gravitation (661); Bayesian statistics (1900); Stellar structures (1631); Non-standard theories of gravity (1118); Fundamental parameters of stars (555)

## 1. Introduction

The idea that the Sun can be considered a laboratory for fundamental physics traces back to the early developments in nuclear physics and contributes to our understanding of the basic nuclear processes involved in stellar nucleosynthesis. In recent times, accurate measurements of acoustic  $p$ -mode spectrum combined with inversion techniques have further stressed this role (Basu 2016). Important examples are the investigation of the equation of state (Basu et al. 1999), the discovery of neutrino flavor oscillations (Fukuda et al. 1998; Ahmad et al. 2002), the properties of dark matter (Lopes et al. 2002, 2014; Lopes & Silk 2012; Vincent et al. 2015), the constraints on axions emission (Schlattel et al. 1999b; Vinyoles et al. 2015), the properties of the screening of nuclear reaction rates (Fiorentini et al. 2001; Weiss et al. 2001), and constraints on fundamental constants (Christensen-Dalsgaard et al. 2005).

In particular, in Guenther et al. (1998) a direct comparison of low-degree  $p$ -modes to GONG data allowed  $\dot{G}/G|_{t=t_0} \leq 1.6 \times 10^{-12} \text{ yr}^{-1}$  to be obtained for the first time.

In fact, according to a general argument by Dirac (1938) and Milne (1937) secular variations of  $G$  are expected on a cosmic timescale in order to explain various “large numbers” coincidences. This initial intuition has been further elaborated in Brans & Dicke (1961) and Bergmann (1968), and is now an important ingredient of various scalar-tensor theories (Fujii & Maeda 2003), quantum-gravity inspired models of modified gravity (Bonanno et al. 2004; Smolin 2016), and string theory low-energy models (Gasperini 2008).

In this context a widely used approach to promote the gravitational constant to a dynamical variable is to extend the general relativistic framework in which gravity is mediated by a massless spin-2 graviton, to include a spin-0 scalar field that couples universally to matter fields. Even though the universality of freefall is maintained, theories that predict that the locally measured gravitational constant vary with time often violate the equivalence principle in its strong form. For this reason empirical constraints on  $\dot{G}/G|_{t=t_0}$ , where the dot indicates a derivative with respect to the cosmic time  $t$  and  $t_0$  is the present estimate of the age of the universe, have been obtained in several contexts (Uzan 2011; Peebles 2016). Current limits on  $\dot{G}/G|_{t=t_0}$  span from  $\dot{G}/G|_{t=t_0} = (4 \pm 9) \times 10^{-13} \text{ yr}^{-1}$  obtained from the Lunar Laser Ranging experiment (Williams et al. 2004), to

$-3 \times 10^{-13} < \dot{G}/G|_{t=t_0} < 4 \times 10^{-13} \text{ yr}^{-1}$  from Big Bang nucleosynthesis (BBN; Copi et al. 2004), or  $\dot{G}/G|_{t=t_0} \sim 10^{-12} \text{ yr}^{-1}$  from white dwarfs (García-Berro et al. 2011). Asteroseismic constraints on the old, low-mass star KIC 7970740 have determined  $\dot{G}/G|_{t=t_0} = (2.1 \pm 2.9)10^{-12} \text{ yr}^{-1}$  consistent with no variation of  $G$  on a time span of  $\sim 11$  Gyr (Bellinger & Christensen-Dalsgaard 2019).

Because the mass and the age of the Sun are known with great accuracy, helioseismology can provide alternative constraints on  $\dot{G}/G|_{t=t_0}$ . In fact, the solar luminosity  $L_\odot$  varies as  $\sim G^7$  (degl’Innocenti et al. 1996) so that a monotonically time-increasing Newton’s constant must be compensated for by a systematic decrease of core temperature and a corresponding change in the hydrogen abundance in order to match  $L_\odot$ , the solar radius  $R_\odot$  and the metal to hydrogen abundance ratio  $(Z/X)_\odot$ .

In this work, the “best possible estimate” of 8640 days of low- $\ell$  frequency BiSON data (Broomhall et al. 2009) is used in order to improve the limit obtained by Guenther et al. (1998) of more than one order of magnitude.

## 2. Solar Models with Time-evolving $G$

Our solar models are built using the Catania version of the GARSTEC code (Bonanno et al. 2002; Weiss & Schlattel 2008), a fully implicit 1D code including heavy-elements diffusion and updated input physics. We prescribed the time evolution of the gravitational constant as a power law (Guenther et al. 1998; Uzan 2003)

$$G(t) = G_0 \left( \frac{t_0}{t} \right)^\alpha \quad (1)$$

where  $G_0$  is the value of Newton’s constant according to 2010 CODATA so that  $G_0 = 6.67384 \times 10^{-8} \text{ cm}^3 \text{ g}^{-1} \text{ s}^{-2}$  and  $t_0 = 13.78$  Gyr is the reference age of the universe according to most of  $\Lambda$ CDM estimates. As  $G_0 M_\odot \equiv 1.32712440 \times 10^{26} \text{ cm}^3 \text{ s}^{-2}$  (Cox 2000) is fixed,  $M_\odot = 1.98855 \times 10^{33} \text{ g}$  is assumed. Irwin’s equation of state (Cassisi et al. 2003) with OPAL opacities for high temperatures (Iglesias & Rogers 1996) and Ferguson’s opacities for low temperatures (Ferguson et al. 2005) are employed and the nuclear reaction rates are taken from the compilation in Adelberger et al. (2011).

Our starting models are chemically homogeneous pre-main-sequence models with  $\log L/L_\odot = 0.21$  and  $\log T_e = 3638$  K, thus close to the birth line of a  $1 M_\odot$  object. Initial helium fraction,  $(Z/X)$ , and mixing-length parameter are adjusted to match solar radius  $R_\odot = 6.95613 \times 10^{10}$  cm (based on an average of the two values and quoted error bar in Table 3 of Haberreiter et al. 2008) and solar luminosity  $L_\odot = 3.846 \times 10^{33}$  erg s $^{-1}$  (Cox 2000).

In order to estimate the impact of different chemical mixtures, three different abundances and the corresponding OPAL opacities have been considered: Grevesse & Noels (1993; GN) with  $(Z/X)_\odot = 0.0245$ , Grevesse & Sauval (1998; GS) with  $(Z/X)_\odot = 0.0229$ , and the so-called “new abundances” for which  $(Z/X)_\odot = 0.0178$  (Asplund et al. 2009; AS).

The new meteoritic determination of the solar age (Connelly et al. 2012),  $t_\odot = 4.567$  Gyr, has been adopted. This value is in excellent agreement with the helioseismic age in the case of the GN and GS mixture, but not for the AS mixture for which the higher age of  $t_\odot = 4.78$  Gyr is helioseismically preferred (see Bonanno & Fröhlich 2015 for an extended discussion). Therefore, in the AS case both helioseismic and meteoritic ages have been studied.

An average mass loss of  $5 \times 10^{-14} M_\odot \text{ yr}^{-1}$  corresponding to a low-density wind has been adopted. In particular, an initial solar mass of  $1.00025 M_\odot$  has been used in order to match the observed one  $M_\odot$  today.

For actual calculations the following  $2 \times 3\text{D}$  parameter space:  $-0.1 \leq \alpha \leq 0.1$  and  $0.97 \leq S/S_0 \leq 1.03$  for the GN, GS, and AS chemical composition has been considered. The proposed  $\alpha$  range generously covers all previous  $\dot{G}/G|_{t=t_0}$  limits obtained by independent methods (Uzan 2003). Concerning the nuclear reaction rate, the  $S/S_0$  interval  $0.97\text{--}1.03$  allows for an up to  $\pm 3\%$  deviation from the recommended  $S_0$  value at zero energy:  $S_{\text{pp}}(0) = (4.01 \pm 0.04) \times 10^{-22}$  keV b in Adelberger et al. (2011). Note that at variance with previous investigation aimed to determine  $S$  from helioseismology (Antia & Chitre 1999; Schlattl et al. 1999a), the considered  $\pm 3\%$  deviation from the recommended value allows to study the impact of the  $S$  prior on testing the hypothesis  $\alpha \neq 0$ .

### 3. Methods

As a seismic diagnostic the following separation ratios were used:

$$r_{01}(n) = \frac{\nu_{n-1,0} - 4\nu_{n-1,1} + 6\nu_{n,0} - 4\nu_{n,1} + \nu_{n+1,0}}{\nu_{n,1} - \nu_{n-1,1}}$$

$$r_{02}(n) = \frac{\nu_{n,0} - \nu_{n-1,2}}{\nu_{n,1} - \nu_{n-1,1}}, \quad r_{13}(n) = \frac{\nu_{n,1} - \nu_{n-1,3}}{\nu_{n+1,0} - \nu_{n,0}}. \quad (2)$$

These quantities are mostly sensitive to the inner layers of a Sun-like star (Roxburgh & Vorontsov 2003) and in the limit  $n \gg 1$  the following asymptotic expansion holds,

$$r_{\ell,\ell+2}(n) \approx -(4\ell + 6) \frac{1}{4\pi^2 \nu_{n,\ell}} \int_0^{R_\odot} \frac{dc_s}{dR} \frac{dR}{R}. \quad (3)$$

Relation (3) explicitly shows that a change in temperature ( $T$ ) and mean molecular weight ( $\bar{\mu}$ ) directly impacts via the sound speed ( $c_s$ ) on the  $r_{\ell,\ell+2}(n)$  terms as  $\delta c_s/c_s \approx \frac{1}{2} \delta T/T - \frac{1}{2} \delta \bar{\mu}/\bar{\mu}$ . On the other hand, for a large but finite  $n$  different combinations of the ratios in (2) probe the stellar interior differently. In order to better clarify this point it is convenient to follow OtiFloranes et al. (2005) and study the associated

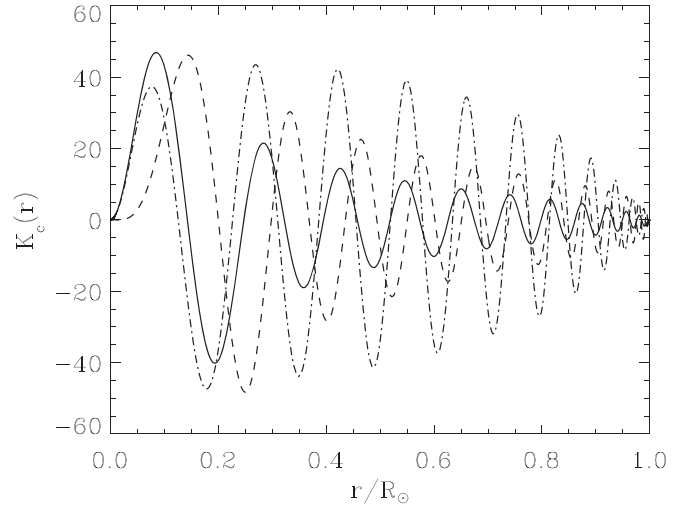


**Figure 1.** Kernel  $K_c$  as a function of the radial coordinate, for the three small separations  $r_{02}$  (solid),  $r_{13}$  (dashed), and  $r_{01}$  (dotted–dashed) for the mode  $n = 10$ .

kernels  $K_c(r)$  and  $K_\rho(r)$ . As displayed in Figure 1 all the kernels are suppressed near the surface, albeit in a different way. The  $r_{02}$  kernel and  $r_{13}$  are clearly more localized near the center than  $r_{01}$ ;  $r_{02}$  in particular can be more suited to study the inner part of core where the nuclear energy production is more efficient.

Moreover, as shown in Doğan et al. (2010), at variance with small frequency-separation (difference), the use of frequency-separation ratios is rather insensitive to the value of the adopted solar radius. We computed the frequencies from the models using the GYRE code (Townsend & Teitler 2013) and the frequency-separation ratios from the computed frequencies.

In order to obtain the frequency-separation ratios the solar-cycle corrected BiSON data presented in Broomhall et al. (2009) were used. Assuming that the errors on the observed frequencies are uncorrelated, the corresponding errors of the separation ratios including the correlations between them could be determined by means of Monte Carlo (MC) simulations. After several MC runs consisting of  $10^8$  trials, the maximal correlation coefficient  $|r|$  turned out to be  $|r| > 1.96 \times 10^{-4}$  with 5% probability and  $|r| > 2.58 \times 10^{-4}$  with 1% probability. Because of this, any cross-correlation terms have been neglected in the likelihood

$$\mathcal{L}(\alpha, S) = \prod_{i=1}^N \frac{1}{\sqrt{2\pi} \sigma_i} \exp\left(-\frac{(d_i - m_i(\alpha, S))^2}{2\sigma_i^2}\right), \quad (4)$$

where  $d_i = r_{l_1 l_2}(n)$  are the observed data ( $n = i + 8$ ,  $i = 1 \dots N$ ,  $N \leq 19$ ),  $m_i$  the theoretical model values, and  $\sigma_i$  the errors.

### 4. Results

In the Bayesian approach the posterior probability distribution is the likelihood (4) weighted with a prior distribution. Obviously, this prior distribution should be a flat one with respect to  $\alpha$ . Concerning  $S/S_0$  we decided to take a conservative point of view, i.e., that within  $0.97 \leq S/S_0 \leq 1.03$  no value is preferred. In that case we are on the safe side and the only eligible prior distribution is a flat one over the logarithm,  $\ln(S/S_0)$ . It turns out that the posterior probability distribution is nearly indistinguishable from a

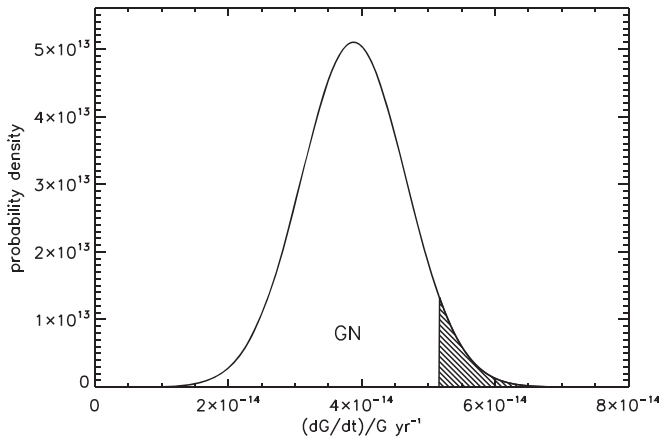


**Figure 2.** Marginal distribution and upper 95% limit for the **GN** mixture taking into account all available diagnostics.

2D Gaussian in the  $\alpha - \ln(S/S_0)$  plane. The reason is that the theoretical models, i.e., the  $m_i(\alpha, \ln(S))$ , are for small deviations linearly dependent on both  $\alpha$  and  $\ln(S/S_0)$  (see O’Hagan & Forster 2004).

We also found that in case of the  $r_{02}$  and  $r_{13}$  diagnostics  $\alpha$  and  $\ln(S/S_0)$  are anti-correlated, i.e., the more negative  $\alpha$  the more positive  $\ln(S/S_0)$ . The contrary holds for the  $r_{01}$  diagnostics. These (net) correlations are caused by a degeneration in the  $\alpha - \ln(S/S_0)$  parameter space: given a linear dependency  $m_i(\alpha, S)$  on  $\alpha$  and  $\ln(S/S_0)$ , one can almost always play off an  $\alpha$  change by an appropriate change of  $\ln(S/S_0)$ . That behavior is dependent on radial mode  $n = i + 8$ . Considering many modes means that the degeneracies are smeared out. The remaining correlations are therefore merely net ones.

The advantage of the Bayesian approach is hypothesis testing. One can compare *quantitatively* the hypothesis  $H_1 = H_1(-0.1 \leq \alpha \leq 0.1, 0.97 \leq S/S_0 \leq 1.03)$  against the zero hypothesis  $H_0(\alpha = 0, 0.97 \leq S/S_0 \leq 1.03)$ . Integrating the posterior over the whole parameter space or subsections of it, respectively, one gets the required evidences. The ratio of the evidences is what matters. The so-called Bayes factor (BF) measures how many times  $H_1$  out-classes  $H_0$ .

The following results are gained by marginalization, i.e., integrating the posterior density distributions over  $\ln(S/S_0)$ , thereby reducing the dimension of the parameter space. From now on we discuss the marginal distribution over  $\alpha$  or  $\dot{G}/G|_{t=t_0} = -\alpha/t_0$ , respectively (see Figure 2).

It is instructive to discuss the results for the three diagnostics  $r_{01}$ ,  $r_{02}$ , and  $r_{13}$  separately as well as the combination of up to three diagnostics as displayed in Table 1 where we have done it for the chemical mixtures considered, **GN**, **GS**, and **AS**.

Unfortunately, the different diagnostics lead to well-separated posterior distributions in the  $\alpha - \ln(S/S_0)$  parameter space. Strictly speaking, they are—perhaps with the exception of the **GN** case—mutually exclusive. Combining up to three diagnostics by multiplying the posteriors requires looking at the local maximum within the intersection region, which has from the outset a rather low probability density. Therefore, the right columns of Tables 1 and 2 should be considered with caution.<sup>3</sup>

<sup>3</sup> Unless one is fond of Arthur Conan Doyle’s famous conclusion: “When you have excluded the impossible, whatever remains, however improbable, must be the truth (Doyle 1892, *The Strand Magazine*).”

**Table 1**

Bayes Factors (BF) and (the Line Below) 95% Limits for  $\dot{G}/G|_{t=t_0}$  in  $\text{yr}^{-1}$  Delineated from the Marginal Probability Distributions Over  $\alpha$  (See Figure 2)

Diagnostics			Up to Three Diagnostics Combined
$r_{01}$	$r_{02}$	$r_{13}$	
		<b>GN</b> composition	
BF $\ll 1$	32 $17 \times 10^{-14}$	BF $\ll 1$	300 $5.2 \times 10^{-14}$
		<b>GS</b> composition	
BF $\ll 1$	$1.7 \times 10^{10}$ $23 \times 10^{-14}$	66 $-19 \times 10^{-14}$	BF $\leq 1$
		<b>AS</b> composition	
...	$2 \times 10^{31}$ $\sim 42 \times 10^{-14}$	BF $\ll 1$	$3.5 \times 10^6$ $18 \times 10^{-14}$

**Note.** Shown are only results where the hypothesis  $H_1$  out-classes the zero hypothesis  $H_0(\alpha = 0)$ , i.e., BF  $> 1$ . In the **AS**- $r_{02}$  case the distribution function is cut due to missing data for  $\alpha < -0.006$ . The right column shows what happened when all available diagnostics are formally combined.

**Table 2**

As Table 1 but Assuming Instead of a Flat Prior a Gaussian One Over  $\ln(S/S_0)$  with Dispersion of 0.01, i.e., as Large as  $S_{pp}(0)$ ’s Relative Error (Adelberger et al. 2011)

Diagnostics			Up to Three Diagnostics Combined
$r_{01}$	$r_{02}$	$r_{13}$	
		<b>GN</b> composition	
BF $\ll 1$	28 $16 \times 10^{-14}$	BF $\ll 1$	190 $5.1 \times 10^{-14}$
		<b>GS</b> composition	
BF $\ll 1$	$8.3 \times 10^8$ $23 \times 10^{-14}$	250 $-17 \times 10^{-14}$	BF $\leq 1$
		<b>AS</b> composition	
...	$5.7 \times 10^{31}$ $41 \times 10^{-14}$	BF $\ll 1$	$5.5 \times 10^7$ $16 \times 10^{-14}$

In order to get a glimpse how the  $\ln(S/S_0)$  prior shapes the outcome, Table 2 shows the corresponding results for a Gaussian prior with a dispersion of 0.01, i.e., the  $S$ -factor’s relative error as given in Adelberger et al. (2011). Obviously, the influence of the prior is negligible.

Concerning the **AS** case: although for models with higher solar age the goodness-of-fit, expressed as the minimum of  $\chi^2 = \sum_{i=1}^N (d_i - m_i(\alpha, S))^2 / \sigma_i^2$ , is comparable with that of the two other compositions (**GN** and **GS**), the radius of the base of the convection zone  $R_{CZ}/R_\odot = 0.721$  and the surface helium abundances  $Y_{\text{surf}} = 0.236$  are in conflict with helioseismic data ( $R_{CZ}/R_\odot = 0.713 \pm 0.001$ ,  $Y_{\text{surf}} = 0.2485 \pm 0.0035$ ; Serenelli et al. 2009) at  $8\sigma$  and  $3.6\sigma$ , respectively. If one instead tries to fit the **BiSON** derived frequency separations with the **AS** composition *and* insisting on an age of 4.567 Gyr, one does not get an acceptable fit at all. The average deviation exceeds in all tested<sup>4</sup> cases the errors  $\sigma_i$  at least ten-fold. For the above reasons, we conclude that it is not possible to extract any compelling conclusion using the **AS** mixture.

<sup>4</sup> For these  $\chi^2$  tests  $\ln(S/S_0) = 0 \pm 0$  has been assumed, i.e., the standard  $S$ -factor.

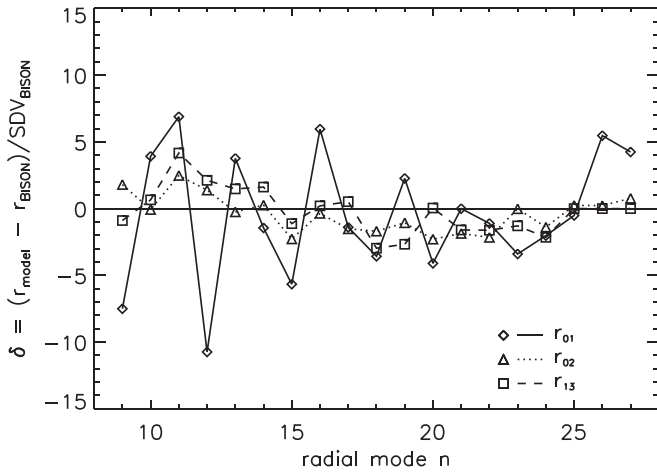


**Figure 3.** Deviation of the theoretical separation ratios from the ones derived from the BiSON data in units of the standard deviation as a function of the radial mode number  $n$ . Shown is the best-fit case for GN composition, with flat prior and all three diagnostics combined (see Table 1 and Figure 2), i.e.,  $\alpha = -0.000534$  and  $\ln(S/S_0) = 0.0206$ . The  $\chi^2$  sums up to 516, which corresponds to an average deviation of  $3.1\sigma$ . As already mentioned the combined posterior leads to a rather poor fit.

As an example Figure 3 depicts the goodness-of-fit performance for the GN case with three diagnostics being combined (Table 1). The deviations expressed in units of the error depend strongly on radial number. For this model we found  $R_{CZ}/R_{\odot} = 0.713$  and  $Y_{\text{surf}} = 0.2467$  in agreement with helioseismology.

With regard to the  $\chi^2$  criterion—albeit technically extraneous to our Bayesian approach—only the  $r_{02}$  cases with GN and GS composition in Table 1 provide acceptable fits at all.

## 5. Conclusions

The most restrictive upper bound,  $\dot{G}/G|_{t=t_0} < 5.2 \times 10^{-14} \text{ yr}^{-1}$  (see Figure 2), comes from combining all available GN diagnostics. Its BF of 300 is comparable with a  $5\sigma$  effect. As already stressed it arises from lumping together three diagnostics, with two of them being fully consistent with the zero hypothesis. For this reason, in order to be on the safe side we therefore prefer the upper bound of  $\dot{G}/G|_{t=t_0} < 17 \times 10^{-14}$  resulting from the  $r_{02}$  diagnostics in the case of the GN mixture. In fact, as shown in Figure 1 the  $r_{02}$  diagnostics is best suited to study the inner core.

One should note that the  $r_{13}$  diagnostics is always in favor of negative  $\dot{G}/G$ . In the GS case this is even significant as the BF of 66 (Table 1) and 250 (Table 2) demonstrates.

Altogether, assuming that the  $S$ -factor represents the biggest and only uncertainty in modeling the Sun, admitting that the different diagnostics,  $r_{01}$ ,  $r_{02}$ , and  $r_{13}$ , result in different upper 95% limits, and taking into account all the evidences listed in Table 1, our most conservative limit on the variation of the gravitational constant is nevertheless clearly restricted:  $|\dot{G}/G|_{t=t_0} < 2 \times 10^{-13} \text{ yr}^{-1}$ .

This result represents the most tight limit on the variation of  $G$  ever obtained with helioseismology and, in general, it is one of the most stringent limits obtained in the literature on a possible secular variation of the Newton constant.

We acknowledge L. Santagati for careful reading of the manuscript. We also would like to thank the anonymous referee

for important comments and remarks that have greatly improved our analysis. A.B. acknowledges the support from ASI-INAF agreement No. 2015-019-R.1-2018.

## ORCID iDs

Alfio Bonanno  <https://orcid.org/0000-0003-3175-9776>

## References

- Adelberger, E. G., García, A., Robertson, R. G., et al. 2011, *RvMP*, **83**, 195  
 Ahmad, Q. R., Allen, R. C., Andersen, T. C., et al. 2002, *PhRvL*, **89**, 011301  
 Antia, H. M., & Chitre, S. M. 1999, *A&A*, **347**, 1000  
 Asplund, M., Grevesse, N., Sauval, A. J., & Scott, P. 2009, *ARA&A*, **47**, 481  
 Basu, S. 2016, *LRS*, **13**, 2  
 Basu, S., Däppen, W., & Nayfonov, A. 1999, *ApJ*, **518**, 985  
 Bellinger, E. P., & Christensen-Dalsgaard, J. 2019, *ApJL*, **887**, L1  
 Bergmann, P. G. 1968, *IJTP*, **1**, 25  
 Bonanno, A., Esposito, G., & Rubano, C. 2004, *CQGr*, **21**, 5005  
 Bonanno, A., & Fröhlich, H.-E. 2015, *A&A*, **580**, A130  
 Bonanno, A., Schlattl, H., & Paternò, L. 2002, *A&A*, **390**, 1115  
 Brans, C., & Dicke, R. H. 1961, *PhRv*, **124**, 925  
 Broomhall, A.-M., Chaplin, W. J., Davies, G. R., et al. 2009, *MNRAS*, **396**, L100  
 Cassisi, S., Salaris, M., & Irwin, A. W. 2003, *ApJ*, **588**, 862  
 Christensen-Dalsgaard, J., Di Mauro, M. P., Schlattl, H., & Weiss, A. 2005, *MNRAS*, **356**, 587  
 Connelly, J. N., Bizzarro, M., Krot, A. N., et al. 2012, *Sci*, **338**, 651  
 Copi, C. J., Davis, A. N., & Krauss, L. M. 2004, *PhRvL*, **92**, 171301  
 Cox, A. N. 2000, *Allen's Astrophysical Quantities* (Berlin: Springer)  
 degl'Innocenti, S., Fiorentini, G., Raffelt, G. G., Ricci, B., & Weiss, A. 1996, *A&A*, **312**, 345  
 Dirac, P. A. M. 1938, *RSPSA*, **165**, 199  
 Doğan, G., Bonanno, A., & Christensen-Dalsgaard, J. 2010, in *HELAS IV Int. Conf.*, 2010, *Astronomische Nachrichten*, ed. S. Jiménez, P. Pallé Pere, & T. Roca (New York: Wiley) arXiv:1004.2215  
 Ferguson, J. W., Alexander, D. R., Allard, F., et al. 2005, *ApJ*, **623**, 585  
 Fiorentini, G., Ricci, B., & Villante, F. L. 2001, *PhLB*, **503**, 121  
 Fujii, Y., & Maeda, K. 2003, *The Scalar-Tensor Theory of Gravitation*, Cambridge Monographs on Mathematical Physics (Cambridge: Cambridge Univ. Press)  
 Fukuda, Y., Hayakawa, T., Ichihara, E., et al. 1998, *PhRvL*, **81**, 1562  
 García-Berro, E., Lorén-Aguilar, P., Torres, S., Althaus, L. G., & Isern, J. 2011, *JCAP*, **5**, 021  
 Gasperini, M. 2008, *LNP*, **737**, 787  
 Grevesse, N., & Noels, A. 1993, in *Conf. Ser.* 245, *Origin and Evolution of the Elements*, ed. N. Prantzos, E. Vangion-Flam, & M. Casse, **14**  
 Grevesse, N., & Sauval, A. J. 1998, *SSRv*, **85**, 161  
 Guenther, D. B., Krauss, L. M., & Demarque, P. 1998, *ApJ*, **498**, 871  
 Haberreiter, M., Schmutz, W., & Kosovichev, A. G. 2008, *ApJL*, **675**, L53  
 Iglesias, C. A., & Rogers, F. J. 1996, *ApJ*, **464**, 943  
 Lopes, I., Panci, P., & Silk, J. 2014, *ApJ*, **795**, 162  
 Lopes, I., & Silk, J. 2012, *ApJ*, **757**, 130  
 Lopes, I. P., Silk, J., & Hansen, S. H. 2002, *MNRAS*, **331**, 361  
 Milne, E. A. 1937, *Natur*, **139**, 409  
 O'Hagan, A., & Forster, J. J. 2004, *Kendall's Advanced Theory of Statistics: Bayesian Inference*, Vol. 2B (2nd ed.; London: Holder Arnold)  
 OtiFloranes, H., Christensen-Dalsgaard, J., & Thompson, M. J. 2005, *MNRAS*, **356**, 671  
 Peebles, P. J. E. 2016, *EPJH*, **42**, 177  
 Roxburgh, I. W., & Vorontsov, S. V. 2003, *A&A*, **411**, 215  
 Schlattl, H., Bonanno, A., & Paternò, L. 1999a, *PhRvD*, **60**, 113002  
 Schlattl, H., Weiss, A., & Raffelt, G. 1999b, *Aph*, **10**, 353  
 Serenelli, A. M., Basu, S., Ferguson, J. W., & Asplund, M. 2009, *ApJL*, **705**, L123  
 Smolin, L. 2016, *CQGr*, **33**, 025011  
 Townsend, R. H. D., & Teitler, S. A. 2013, *MNRAS*, **435**, 3406  
 Uzan, J.-P. 2003, *RvMP*, **75**, 403  
 Uzan, J.-P. 2011, *LRR*, **14**, 2  
 Vincent, A. C., Scott, P., & Serenelli, A. 2015, *PhRvL*, **114**, 081302  
 Vinyoles, N., Serenelli, A., Villante, F. L., et al. 2015, *JCAP*, **10**, 015  
 Weiss, A., Flaskamp, M., & Tsytoch, V. N. 2001, *A&A*, **371**, 1123  
 Weiss, A., & Schlattl, H. 2008, *Ap&SS*, **316**, 99  
 Williams, J. G., Turyshv, S. G., & Boggs, D. H. 2004, *PhRvL*, **93**, 261101